



## Influence of the silicon content on the high temperature oxidation of a spheroidal graphite cast iron. part 2: Oxidation behaviour of the SG cast iron samples versus their SI content

Mamadou Saidou Diallo<sup>1,2</sup>, Lionel Aranda<sup>3</sup>, Pascal Villeger<sup>3</sup>, Patrice Berthod<sup>1,2,3\*</sup>, Elodie Conrath<sup>1,2,3</sup>

<sup>1</sup>University of Lorraine, (FRANCE)

<sup>2</sup>Faculty of Sciences and Technologies, (FRANCE)

<sup>3</sup>Institut Jean Lamour (UMR 7198), Team 206 "Surface and Interface, Chemical Reactivity of Materials"

B.P. 70239, 54506 Vandoeuvre-lès-Nancy, (FRANCE)

E-mail : Patrice.Berthod@univ-lorraine.fr

### ABSTRACT

In this second part of the work the re-melted then re-solidified spheroidal graphite (SG) cast iron samples, without or with enrichment in silicon, were exposed to high temperature (rather fast heating, 10 minutes at 957°C, very slow cooling) in air. Concerning the surface state all the samples were oxidized, with the exclusive formation of Fe<sub>2</sub>O<sub>3</sub>. The oxide scales were about 20-25 μm thick and a graphite-free zone developed from the external surface over an about 60-70 μm depth. The silicon had a lowering influence on these two parameters, clearly for the first one but not so clear for the second one. Concerning the bulk the thermal cycle applied was largely sufficient to correct the matrix microstructure since all primary cementite and pearlite have disappeared. The influence of these silicon contents and these heat-treatment parameters remains to be tested for much coarser microstructures of SG cast irons. © 2015 Trade Science Inc. - INDIA

### KEYWORDS

Spheroidal graphite  
cast iron;  
Silicon;  
High temperature oxidation.

### INTRODUCTION

Cast irons<sup>[1,2]</sup> are iron-carbon alloys among the easiest to shape by foundry. Their good castability is due to a melting temperature range rather low by comparison to steels. Indeed, as readable in the binary Fe-C diagrams<sup>[3]</sup> the presence of about 4.25 wt.% of carbon leads to a fall in melting temperature from 1535°C for pure Fe down to 1153°C in the austenite-graphite stable diagram and 1147°C in the austenite-cementite metastable diagram. Cast irons are furthermore rather cheap

iron-based alloys since there is no compulsory to remove the carbon from liquid metal cyclically getting out of the blast furnace as for steels. Cast irons shaped by moulding directly after they leaved the bottom part of the blast furnace<sup>[4]</sup> are also naturally rich in silicon. Indeed, since the reduction of layers of iron ore by first CO/CO<sub>2</sub> gases "generated by the combustion of coke in the bottom of the blast furnace – in the upper part of this one (i.e. the indirect reduction, Fe<sup>III</sup>O<sub>3</sub><sup>(solid)</sup> → Fe<sup>II</sup>O<sup>(solid)</sup>) followed by the direct reduction of liquid iron oxide in contact with the coke parts (present as

layers alternated with the ore ones) according to  $\text{Fe}^{\text{II}}\text{O}^{\text{(solid)}} \rightarrow \text{Fe}^{\text{(liquid)}}$ , is accompanied by the reduction of silica too  $\text{SiO}_2 \rightarrow \text{Si}^0$  (silica coming from the ore gangue) by the same carbon-rich species. Thanks to the “clean” chemical compositions (i.e. almost no other elements than Fe, Si and C, at least in significant quantities) of the pig iron (cast iron resulting directly from ore reduction) pieces fabricated just downstream of the blast furnace solidify according to the austenite-graphite diagram if the solidification is not too fast. The solidification microstructure is then composed of austenite (pre-eutectic dendrites and eutectic, or only eutectic) and graphite (eutectic or re-eutectic and eutectic), depending on the position of the equivalent carbon content  $\{ \text{wt.}\% \text{C} + (\text{wt.}\% \text{Si} + \text{wt.}\% \text{P})/3 \}$  relative to the eutectic value. If the solid state cooling rate is itself not too fast, the eutectoid solid state transformation of austenite near  $800^\circ\text{C}$  results in ferrite and additional graphite. Without any treatment of the liquid metal prior to pouring in mould and solidification, the shape of the obtained graphite is lamellar (“flake graphite”). It is coarse in case of slow solidification or finer if solidification was more rapid and/or if inoculation of the liquid metal was carried out before or during pouring. The liquid metal may be treated by a first desulfurization (e.g. with CaO) to remove the greatest part of sulphur coming from the iron or in the blast furnace, second by powdered magnesium-rich FeSi alloy or by immersion of blocks of pure magnesium, to purify (down to less than at least 0.010 wt.%) the liquid iron in sulphur, oxygen and other elements acting as poisons for spheroidal growth of graphite. Finally, after inoculation with a FeSi powder containing nuclei for graphite (and sometimes rare earth elements), the graphite particles crystallize as spheroids<sup>[6]</sup>. Such graphite shape is much less detrimental for the mechanical properties of the obtained cast irons than flake graphite and high strength and ductility may be obtained. The overall mechanical properties may be thereafter rated by heat-treatments to modify the matrix. For instance austenitization can be carried out at about  $1000^\circ\text{C}$ , followed by either faster cooling to obtain ferritic-pearlitic or wholly pearlitic matrix, or quenching (eventually followed by ageing) for obtaining bainitic matrix (austempered ductile iron) or martensite.

However, in some case of too low contents in

“graphitizing” elements (e.g. Si) and/or local too fast cooling (thin part of the pieces, edge...) solidification may involve the two diagrams stable and metastable together<sup>[8]</sup>, with as result a microstructure composed of both graphite and of primary cementite. Since cementite is detrimental for the toughness of the cast iron it may be compulsory to suppress it, by a heat-treatment called “graphitization treatment”. This consists in exposing the piece at a very high temperature (typically  $1000^\circ\text{C}$ ) during several minutes to destabilize cementite which then transforms into austenite and graphite. When such heat-treatment is applied, this is generally in the atmosphere present inside the plant, as is to say air or more or less humidified air. Oxidation phenomena necessarily occurs and since not alloyed cast iron does not contain elements as aluminium or chromium in quantities high enough to allow it resisting high temperature oxidation<sup>[9,10]</sup>, surface oxidation is rather fast since Fe forms not stoichiometric oxides contrarily to Al and Cr. In contrast silicon, which is an element which may form protective oxide scale over refractory materials such as  $\text{MoSi}_2$ , may have a beneficial effect for the behaviour of cast irons.

In this second part it was wished to study the effect of the silicon content on the high temperature oxidation behaviour of a given cast iron during graphitization treatment. For that, three ingots of cast iron with the same microstructure fineness and the same Fe and C contents, but displaying varied contents in Si, were tested in oxidation by air following a thermal cycle typical of a graphitization treatment.

## EXPERIMENTAL

### The studied cast irons

Three ingots of cast iron with 2.5, 3.0 and 3.5wt.% Si were elaborated in the first part of this work<sup>[11]</sup>. This was achieved by high frequency induction heating in argon atmosphere, by re-melting of parts cut in a same initial great ingot of spheroidal SG cast iron in order to add it supplementary silicon before their re-solidification. Their as-cast microstructures are reminded in Figure 1. They are of a hypo-eutectic composition (presence of austenite dendrites become pearlitic) and contain, besides the eutectic cells, pearlite (less for higher Si content) and free ferrite (more for higher Si content).

## Full Paper

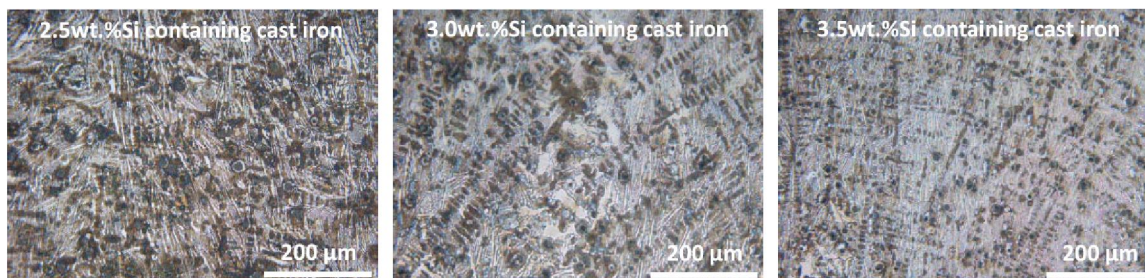


**Figure 1 :** Micrographs illustrating the as-cast microstructures of the re-melted then re-solidified cast irons (Nital 4 etching, optical microscope); the Si content increases from the left micrograph to the right one

### The high temperature oxidation tests

In each ingot several parts were cut using a Buehler Delta Abrasimet disc saw, in order to generate small cubes of about 4mm × 4mm × 4mm. In each ingot a sample was cut in the “top” location, another one in the “middle” location and the last one in the “bottom” location (Figure 2).

The six faces of each of them were ground with 1200-grit SiC-papers all around, with special smoothing of their twelve edges and of their eight corners. They were preliminarily weighed, then placed in the hot zone of a tubular resistive furnace (Carbolite, maximal temperature: 1200°C) where they were heated at +20K min<sup>-1</sup> in laboratory air until reaching 957°C, temperature at which they stood during 10 minutes (temperature and duration both typical of a graphitization treatment). At the end of the 10 min–stage the furnace was shut off and the samples, still in the middle of the furnace, cooled slowly following an hyperbolic temperature variation law.

### Metallography characterization after oxidation test

The samples issued from the oxidation tests were first weighed again to calculate the mass gain per surface unit area. The oxidized surfaces of the samples were thereafter analysed by X-Ray Diffraction (XRD) using a Philips X’Pert Pro diffractometer, to specify the natures of the oxides externally formed. Thereafter they were covered on their six faces by a thin gold layer by cathodic pulverization with a JEOL device, allowing surface observation with a Scanning Electron Microscope JEOL JSM 6010 LA (SEM) in Secondary Electrons (SE) mode. Now electrical conductive on surface the samples were all around covered with a thick layer of electrolytic nickel (2 hours under 50mA in a

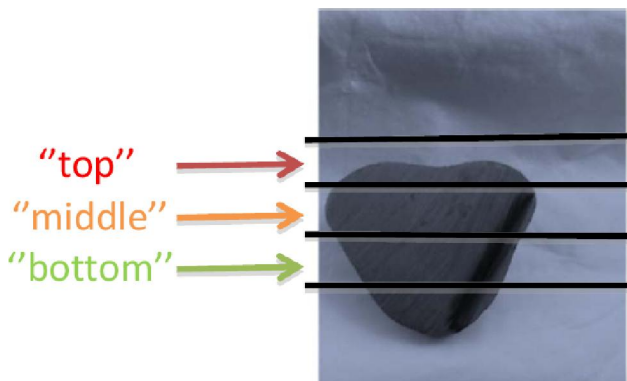


**Figure 2 :** Macrograph of half a re-melted/re-solidified ingot with coloured arrows showing the “top”, “middle” and “bottom” locations where the cubic samples were cut for the oxidation tests

{NiSO<sub>4</sub>·6H<sub>2</sub>O + H<sub>3</sub>BO<sub>3</sub>} aqueous solution heated at 50°C). The oxidized samples thus covered by a protective layer preventing loss of oxide during cutting and grinding, were thereafter sawed in two parts using the disc saw mentioned above and embedded in a cold resin mixture (resin Araldite DBF + hardener HY956, Escil). The mounted samples were ground with SiC-papers from 120 to 1200 grade, under water from 120 up to 800-grit, and without any lubricant for the 1200-grit paper since dry final grinding is compulsory to preserve the graphite nodules from shape deterioration. After an intermediate ultrasonic cleaning the samples were finally polished with textile enriched with 1μm hard particles. The matrixes of the samples were controlled using an Olympus BX51 equipped with a digital camera, after Nital 4 etching (10 seconds of immersion in a 96% ethanol - 4% nitric acid solution). The mounted and polished samples were observed using the SEM in Back Scattered Electrons (BSE) mode. The thicknesses of the external scales were measured as well as the depth over which graphite disappeared from the oxidation front.

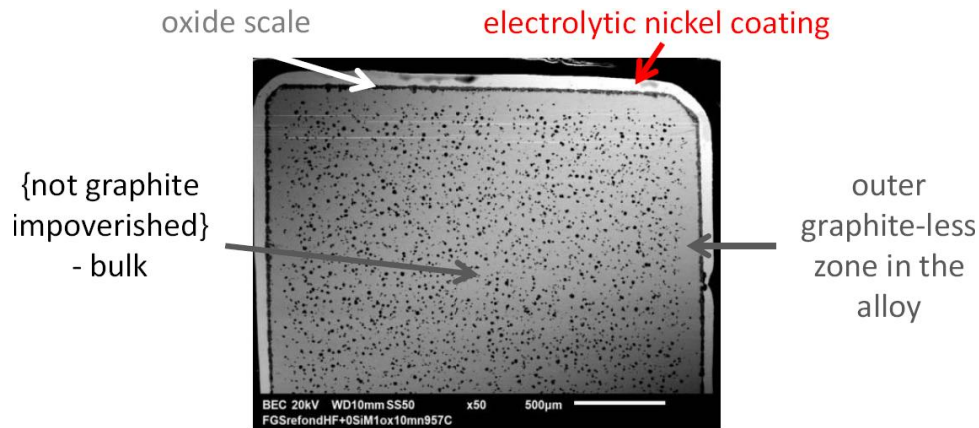


Figure 3 : SEM/BSE macrograph of cross-section metallographic sample

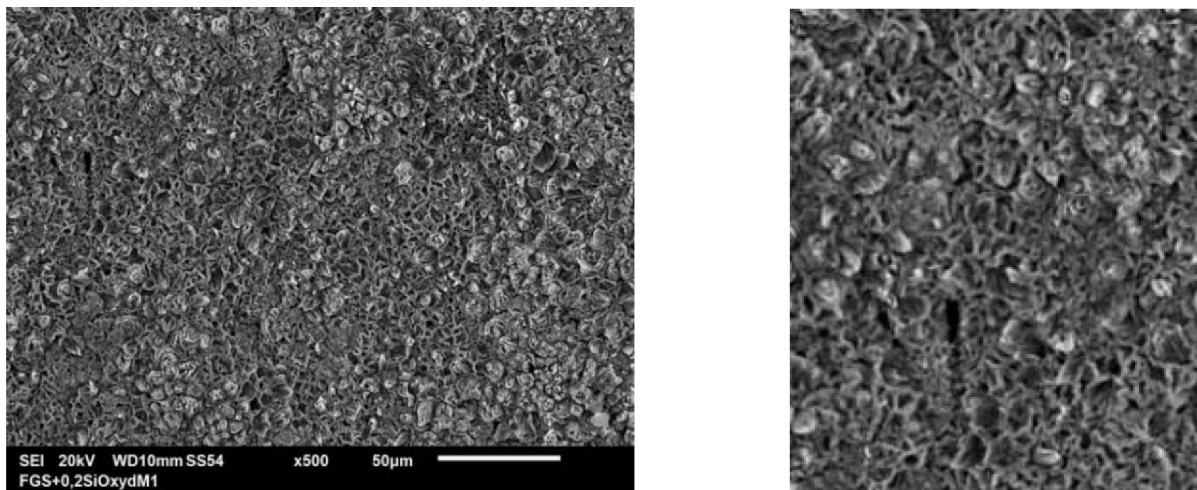


Figure 4 : SEM/SE micrograph of the surface of an oxidized 3.0wt.%Si-containing SG cast iron sample (right: 2× enlargement of a part of the left image)

The macrograph presented in Figure 3 illustrates the metallographic preparation with the view of a cut, embedded and polished Ni-coated oxidized sample, as well as the oxide scale and the graphite-free depth all around the cross section.

### Hardness tests

The hardness of the bulk of all the heat-treated samples was specified. Vickers indentations were carried out on the mounted and polished samples, using a Testwell Wolpert apparatus. In all cases the applied load was 10kg.

## RESULTS AND DISCUSSION

### Surface characterization of the oxidized state of the samples

The SEM/SE micrograph displayed in Figure 4 il-

lustrates the morphology of the external oxide scale for one of the oxidized samples, while the diffractograms presented in Figure 5, Figure 6 and Figure 7 demonstrates that this oxide scale is essentially composed of haematite  $\text{Fe}_2\text{O}_3$ .

### Cross-section characterization of the oxidized state of the samples

The surface and sub-surface states of the samples after oxidation test are illustrated by SEM/BSE micrographs in Figure 8. One can observe the external oxide scale in its whole thickness and discover that there is an external part in the sample in which graphite has obviously disappeared.

The average thickness of the external oxide scale and the average depth in which graphite has disappeared were measured and the results are displayed in TABLE 1. One can see that the silicon content in the SG cast

## Full Paper

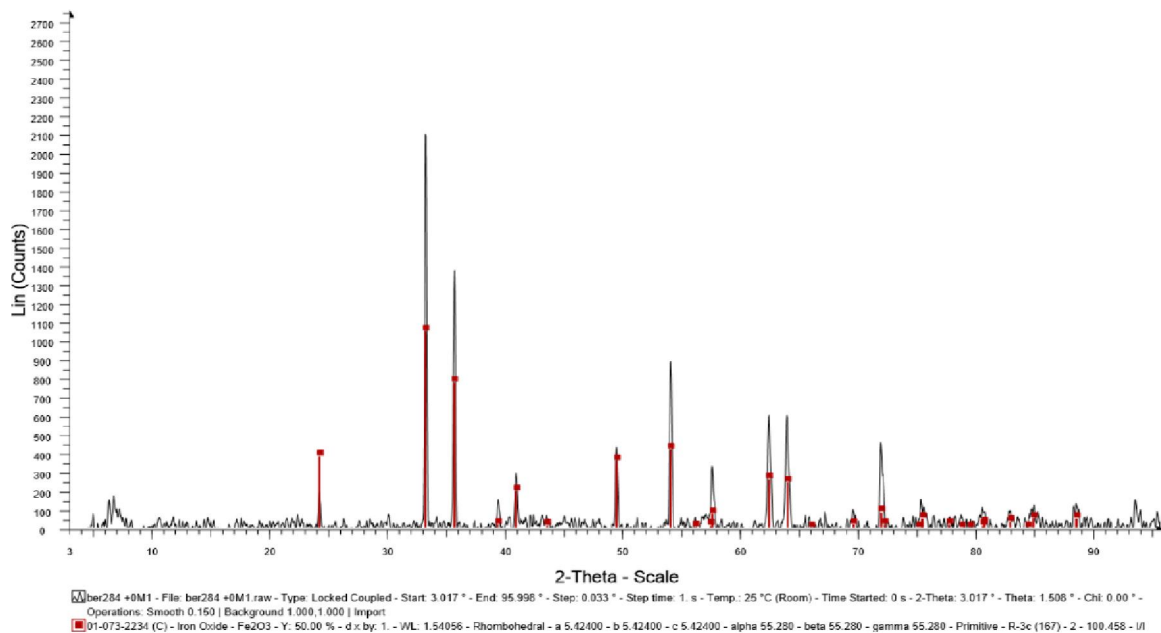


**Figure 5 : XRD spectra acquired on the oxidized surface of a 2.5wt.%Si-containing SG cast iron; indexation showed that  $\text{Fe}_2\text{O}_3$  was the single oxide present (red squares)**

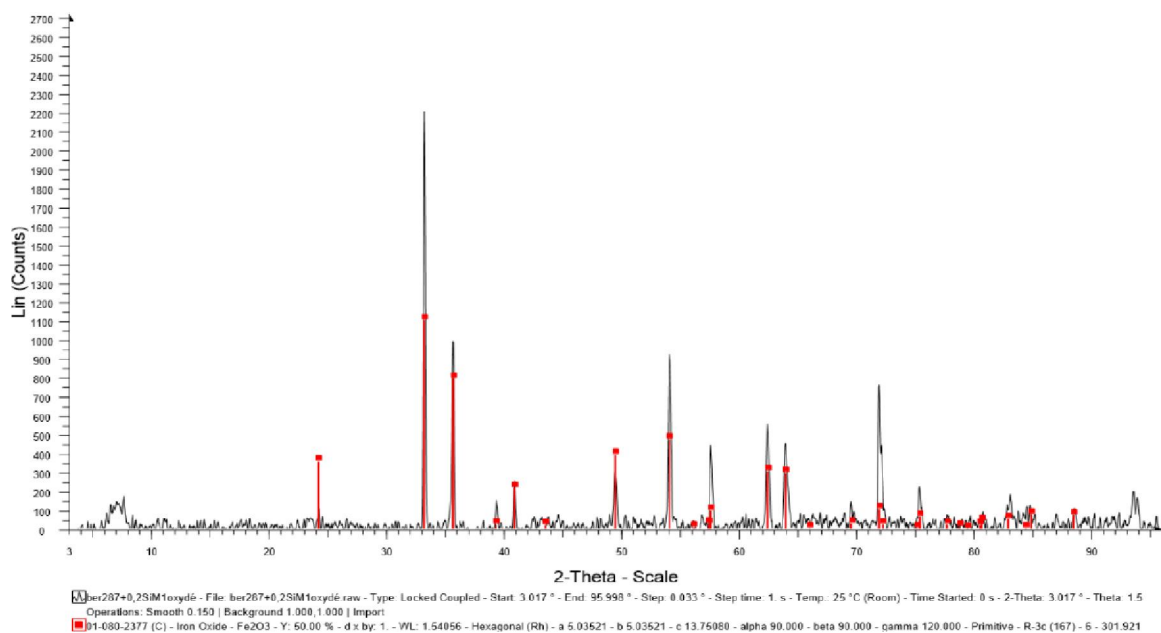


**Figure 6 : XRD spectra acquired on the oxidized surface of a 3.0wt.%Si-containing SG cast iron; indexation showed that  $\text{Fe}_2\text{O}_3$  was the single oxide present (red squares)**

iron sample seems having an effect on both parameters. Indeed, the higher the silicon content, the thinner the external oxide scale. In contrast the depth of the zone in which graphite has disappeared does not show clear evolution with the Si content.

To enrich this evaluation of the dependence of the high temperature oxidation behaviour it was initially wanted to calculate the difference between the initial

mass and the final one after oxidation tests for all samples, and for each of them to divide it by the total external surface of the sample (surfaces measured/calculated before the tests). Unfortunately, 10 minutes did not lead to mass change significant enough (for the micro-balance used) to allow this determination.

Besides, the bulk microstructure was observed using the optical microscope after having etched the pol-

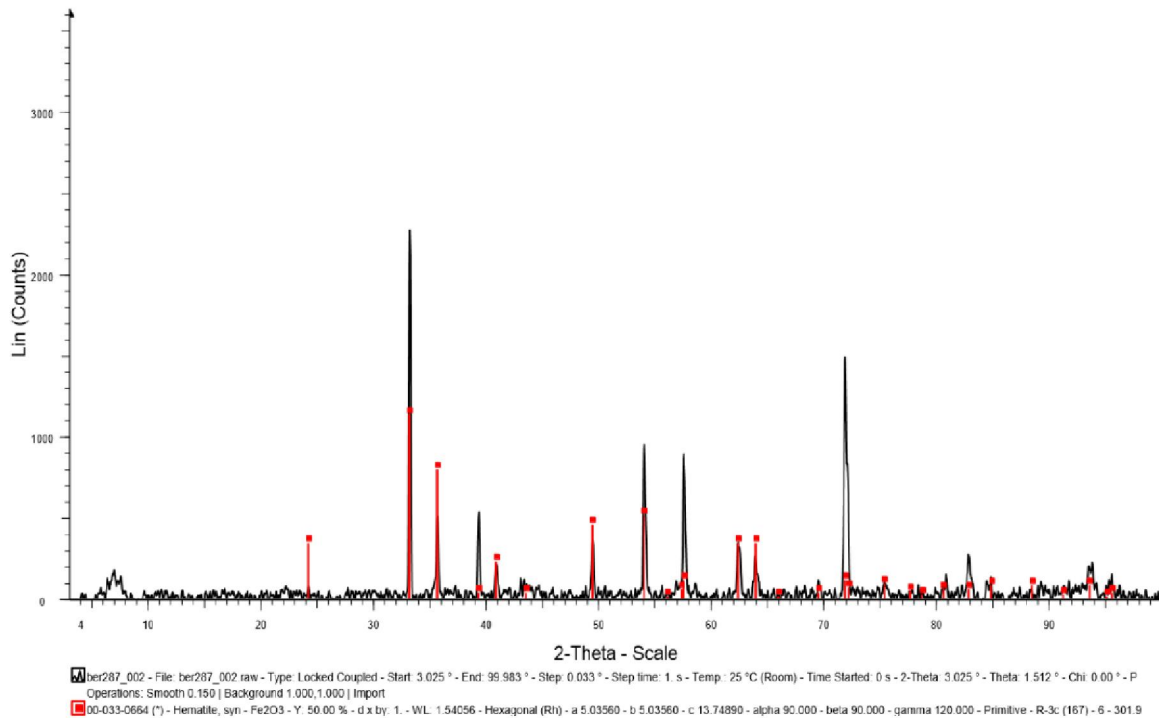


**Figure 7 :** XRD spectra acquired on the oxidized surface of a 3.5wt.%Si-containing SG cast iron; indexation showed that  $\text{Fe}_2\text{O}_3$  was the single oxide present (red squares)

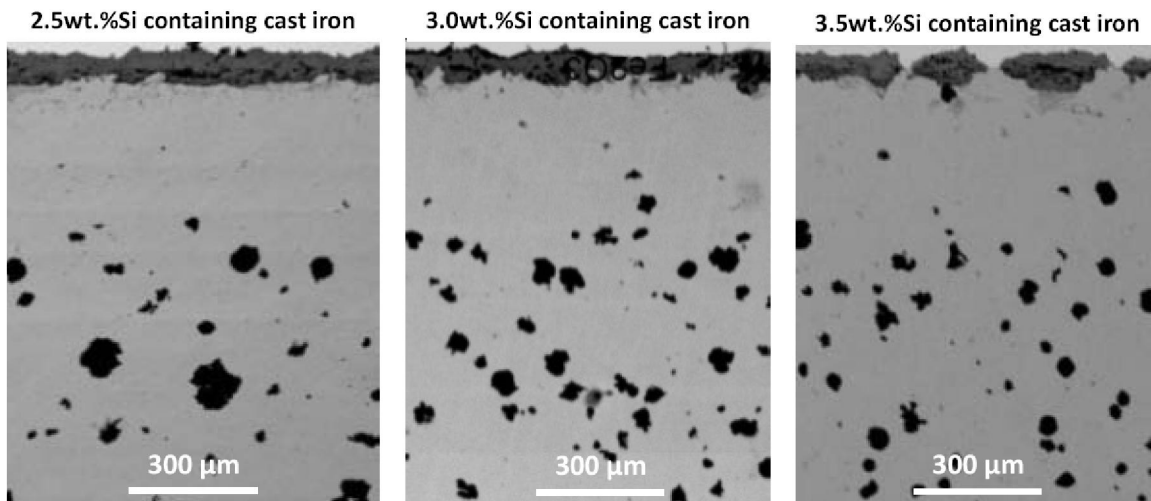


**Figure 8 :** SEM/BSE micrographs illustrating the surface and sub-surface states of the SG cast iron oxidized samples

ished cross section with the Nital solution. It appears that the matrix was totally ferritic in all cases. The heating to 957°C and the following 10 minutes stage were thus sufficient to eliminate all the primary carbides which existed initially after re-solidification in the HF induction furnace. The cooling down to room temperature was also obviously slow enough to favour the {ferrite, graphite} eutectoid transformation instead the pearlitic one. Therefore it was unfortunately not possible to reveal the effect of the Si content on the ferrite/pearlite

ratio after return to room temperature.

### Hardness results

The harness measurements led to the values displayed in TABLE 2. The values are all much lower than the initial ones, what can be easily explained by a matrix become totally ferritic while pearlite and some primary carbides were present before the thermal exposure.

However one can additionally notice that the average hardness tends to increase with the silicon content.

## Full Paper

TABLE 1 : The average values of the thickness of external oxide and of the graphite-free depth

Silicon weight content in the SG cast iron samples	Average oxide scale thickness ( $\mu\text{m}$ )	Average graphite-free depth ( $\mu\text{m}$ )
2.5 wt.%Si	24	70
3.0 wt.%Si	19	60
3.5 wt.%Si	20	65

TABLE 2 : Hardness values obtained for the SG cast iron samples' bulks after high temperature exposure

Silicon weight content in the SG cast iron samples	Localization of the indentations	Values (Hv10kg)	
		When as-cast (reminded <sup>11</sup> )	After heat-treatment
2.5 wt.%Si	top	464	162
	middle	488	151
	bottom	525	151
3.0 wt.%Si	top	450	156
	middle	483	167
	bottom	514	170
3.5 wt.%Si	top	401	189
	middle	478	187
	bottom	336	186

This is due to the wellknown hardening effect of silicon in ferritic iron. One can furthermore remind that too high silicon content in a ferritic iron threatens its ductility, by rising its ductile-brittle transition temperature. This one can even reach the ambient temperature for too present silicon (e.g. 4-5 wt.%).

### General commentaries

The applied thermal cycle was obviously very efficient to suppress primary cementite and pearlite in the SG cast iron samples. It is furthermore probable that either temperature or duration, or both of them may be lowered without changing the result. In another field the samples were significantly deteriorated by hot oxidation, but not necessarily with properties diminution since the most remarkable effect was the graphite loss in sub-surface, as is to say the local replacement of a ferritic SG cast iron by a ferritic steel, i.e. no difference (except a local refractoriness much improved!). It is true that if the duration was much longer the iron consumption by oxidation should be much more severe, but obviously the applied heat-treatment is already over dimensioned for what was demanded to it. Even with its initial content of 2.5 wt.% silicon was present in quantity high enough to help destabilizing cementite during the high temperature stage and to avoid pearlitic formation during the cooling. But it is also true that this

cooling was particularly slow (in shut-off furnace) and nor representative of the most encountered industrial conditions. In addition, the microstructure particularly fine resulting from the fast solidification of the cast iron parts in the copper crucible of the HF induction furnace, led to rather small cementite particles, finely structured pearlite (very fine lamellae of cementite and ferrite) and high density of (finer) graphite nodules, which all favour short distances of diffusion. Such results (total disappearance of cementite disappearance and no re-formation of pearlite at cooling) may be not so surely obtained for the same chemical composition and thermal cycle parameters for coarser initial microstructures.

### CONCLUSIONS

The new ferrite-pearlitic SG cast irons elaborated with various silicon contents in the first part of this work were thus all successfully transformed in wholly ferritic cast irons by applying the heat-treatment in consideration here. The microstructure fineness resulting from fast re-solidification was probably a favourable point for that. Future heat-treatments with lower temperature and/or duration may be much better show the effect of the silicon content on the efficiency of these modified heat-treatments on the matrix, but not on the hot oxidation behaviour which was already not really

detrimental here.

### REFERENCES

- [1] J.R.Davis; Cast Irons, ASM International (1996).
- [2] G.Lesoult; Traité des matériaux : Tome 5, Thermodynamique des matériaux : De l'élaboration des matériaux à la genèse des microstructures, Presses Polytechniques et Universitaires Romandes (2010).
- [3] W.F.Gale, T.C.Totemeier; Smithells Metals Reference Book, Elsevier Butterworth-Heinemann, Burlington (2004).
- [4] J.Szekely; Blast furnace technology, Science and Practice, Dekker (1972).
- [5] J.Szekely, J.W.Evans, H.Y.Sohn; Gas-Solid Reactions, Academic Press Inc., New York (1976).
- [6] M.J.Castro-Roman; Etude expérimentale et modélisation de la solidification des pièces coulées en fonte à graphite sphéroïdal : influence de la vitesse de refroidissement et de l'inoculation; Ph.D. Thesis of the Institut National Polytechnique de Lorraine, Ecole Nationale Supérieure des Mines de Nancy (1991).
- [7] M.J.Castro-Roman; Etude expérimentale et modélisation de la solidification des pièces coulées en fonte à graphite sphéroïdal : influence de la vitesse de refroidissement et de l'inoculation, Ph.D. Thesis of the Institut National Polytechnique de Lorraine, Ecole Nationale Supérieure des Mines de Nancy (1991).
- [8] C.Selig; Développement des microstructures et des microségrégations lors de la solidification des fontes : transition de l'eutectique graphitique vers l'eutectique cémentitique, Ph.D. Thesis of the Institut National Polytechnique de Lorraine, Ecole Nationale Supérieure des Mines de Nancy (1994).
- [9] P.Kofstad; High Temperature Corrosion, Elsevier Applied Science (1988).
- [10] D.Young; High Temperature Oxidation and Corrosion of Metals, Elsevier, Amsterdam (2008).
- [11] M.S.Diallo, P.Berthod; Materials Science: An Indian Journal, submitted.